

Supplemental Information.

“Quantifying Amine Permeation Sources with Acid Neutralization: Calibrations and Amines Measured in Coastal and Continental Atmospheres”

[Nathan A. Freshour](#), [Kimberly K. Carlson](#), [Yemissrach A. Melka](#), [Sandra Hinz](#), [Baradan Panta](#), [David R. Hanson*](#)

11 pages, 20 figures.

Summary.

A description of AmPMS sampling arrangement and how the background signals were obtained in the field studies are described in the first two three pages (S1.1 and S1.2). Tests of an acid scrubbing tube and a comparison to the catalytic converter method for removing bases from the sample are described in section 1.3. Response times due to surface interactions of amines with surfaces are discussed next (sections 1.4-1.5) and low reagent ion count rate episodes in the field studies are discussed in 1.6. Calibration for DMSO is discussed in section 2 and measurements of other species by AmPMS in Lewes DE are presented in section 3. Section 4 presents diurnal averages from the Oklahoma campaign and section 5 shows correlation plots from the Lewes study.

Addition of amines to a nucleation flow reactor are described in section 6 along with CFD simulations of the dispersal of the amine into the main flow within the reactor.

Lastly, a tandem titration experiment is presented and the time and temperature dependencies of the permeation rate of select permeation tubes is presented in section 7.

Contents:

S11-5. AmPMS Information

S16. Addition of Base to Flow Reactor and CFD

S17. Permeation tube diagnostics and properties.

SI1. AmPMS Sampling Information

SI1.1 AmPMS Air inlet lines.

AmPMS samples air (~1200 sccm) through a ~4.5 mm ID Teflon tube that is ~3 to 5 m in length. Just before the ionization region, the sample gas passes through a Teflon union adaptor (1/4" to 3/8") then through a Teflon tee and into the glass manifold of the instrument that surrounds the ionization source, the drift region and the mass spectrometer inlet. The tee allows for supplanting the sample gas flow with a flow of catalytically cleaned air to determine instrument background signals (the "zero" procedure). Sample air flows straight through the tee while clean air during a zero makes a right turn (Fig. S1).

The catalytic converter (AmPMS) provides clean air for determining the instrument background levels and also for the ion source, about 40 sccm. This air flows over a vial that contains a dilute HNO₃ aqueous solution (initial HNO₃ concentration of about 5 wt %) that provides water and HNO₃ vapor for the ion source (four 0.9 μCi Am-241 tabs).

The sample gas flow (1200 sccm) and source flow rates are monitored with delta P flow meters (tubes of ~1/16" and 1/32" inner diameter, respectively) where the pressure drops are about 1 and 0.5 kPa, respectively. During sampling of outdoor air through ~5 m of 1/4" OD tubing, the drift region pressure is about 0.2 kPa below ambient pressure. Pressure sensors are piezo type (MPXV7002 or 5004, Freescale semiconductor). The mini-diaphragm pump (HiBlow USA, CD-8-1101) has a free air flow rate of ~13 L/min which is throttled down to 1200 sccm by the catalytic converter and a small tube on the outlet of a three way solenoid valve. This valve is normally set to vent to ambient through this small tube and the size of the tubing is determined such that the source flow rate does not change when the valve is actuated and clean air is sent to recycle through the drift region.

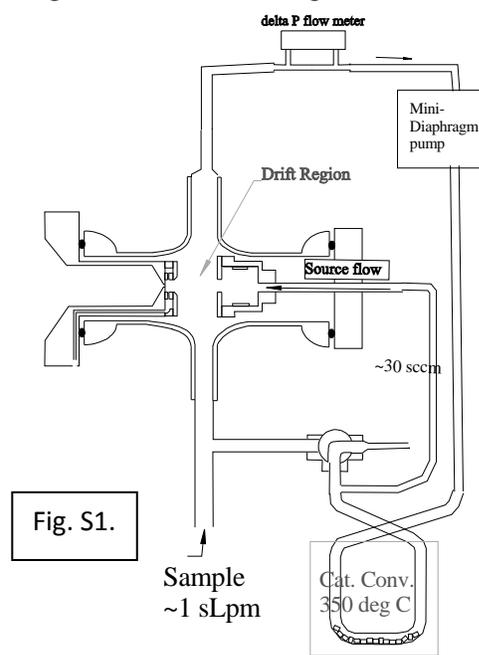


Fig. S1.

Background signals are determined by actuating the valve which initiates a 'zero' where the sample air is replaced by catalytically cleaned air of the same relative humidity. Maintaining a constant relative humidity minimizes changes in background signals. Background signals are also dependent on the temperature of the drift region (monitored with a Tz3.5 X.) A typical zero time period is 20 min and a zero is initiated once every 2 hr.

The curtain gas (*Hanson et al. 2011*) has not been used for the past two AmPMS deployments (July 2012 in Lewes DE and Apr 2013, Purcell, OK.) The advantage is that the instrument does not require pressurized gas cylinders and the curtain gas flow rate has no significant effect on ion detection. The disadvantage is perhaps loss of protection of the orifice from large dust particles or fibers. The pressure on the vacuum system has decreased by 20 to 50 % at times and ion count rates decreased by 50 to 90 % indicating a clog in or near the orifice. Visual verification of the clogs using a microscope was done after the measurement campaigns.

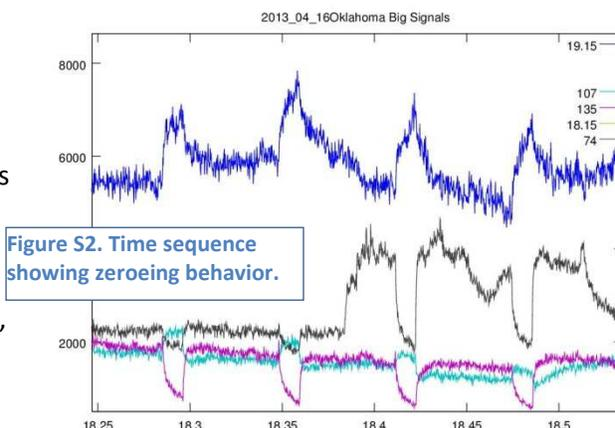
The gas entering the vacuum system comprises about 80-120 sccm which would normally be supplied by clean cylinder gas. However, the recirculating zeroing procedure adopted here leads to a changing RH during a zero if a dry curtain gas is used. Since background signals are sensitive to RH, the curtain gas was eliminated. The recirculating zeroed air does not account for the flow into the vacuum

thus the clean air also entrains about 6-to-10 % raw sample air. The trace gases that AmPMS measures in the sample air vary slowly over time periods of ~ 25 min and this does not significantly affect the data analysis. A new procedure and flow setup that incorporates a second tube for introducing additional air for the curtain gas is planned.

SI1.2 Zeroing behavior

Reliable AmPMS data requires the determination of instrument background signals periodically. This was done every 2 hours by supplanting most of sample gas with recirculating clean gas of the same RH. Temperature, RH, and time all affect the background signal (BG) for most species and extracting abundances for species with large BG are especially vulnerable to its fluctuations. Artifact swings in concentrations can be introduced by quick (~ 1 hr) and large changes in temperature or RH.

The temporal behavior of the amine signals indicated interactions with surfaces. Over time, surfaces in the ion drift region can accumulate material (most likely dust or aerosol particles) and there is evidence that degassing of amines from these surfaces can contribute to the observed signals and cause the instrument response to be sluggish. For example, after the first two weeks of the field campaign in Atlanta (13), the ammonia signal became unusable for deriving ammonia abundances, due to an increased BG level as well as lower NH_3 abundances. BG for NH_3 was not successfully determined at these times; even negative net abundances could be inferred from the data. In the recent Lamont OK campaign this sluggishness was also observed for ammonia and most of the amines. At times swings in abundances resulted in negative values due to inaccurate BGs. The instrument when it was deployed in Lewes DE did not suffer nearly as much from these sluggish intervals.



Normal behavior of AmPMS background determination is depicted in Fig. S2, a plot of signals (Hz at masses: 19.15 u, 74 u, 135 u) vs. UT day for April, 2013. Zeroes are easily seen in the C4-amine data (74 u) and the 135 u data, which is likely a VOC with a high proton affinity, e.g. tetramethyl benzene. During each ~ 20 min zero that occurs about every 2 hrs, the 74 u and 135 u BGs steadily decrease and upon sampling again, rise quickly. Signal for one of the reagent ions, 19 u, shows behavior common to all the reagent ions upon a catalytic zero. Yet changes in the water proton cluster signals that occur during a zero are taken into account in the extracted mixing ratio. The normal procedure for most time periods and most masses is to retain the last third of the zero data as BG. In addition, the first ~ 10 minutes of sample data after each BG is discarded. The mixing ratio for the C4 amine, 74 u, shows good behavior in this sense during this time period. A large increase in this amine occurs at 18.38 d.

However, this normal behavior in BG levels does not always occur for the amines. It is thought that material can accumulate on surfaces within the ion drift region or in the tee just preceding it, which can adversely affect the catalytic zeroing mechanism. There was evidence for occasional minor 'clogs' in the ion sampling orifice: at times there was a severe depletion of reagent ion signals (depletion > 90 %; see SI1.6 below.) This accumulation of material on surfaces led to determining BGs in an alternate manner.

Sluggish behavior in the BGs for dimethyl amine (46 u) is illustrated in Fig. S3a. Dimethyl amine generally had a large BG to signal ratio, with BG mixing ratios equivalent to several hundred pptv at times. Also, the C4-amine at mass 74 u had BG equivalent to a few ppbv at times. Signals are converted to pptv in the figure. Mixing ratios typically decrease upon a zero but during sluggish periods the data, e.g. for 46 u in the figure, initially shows an increase (zero starts at: 21.75 21.83, 21.92) and then falls slowly over the next 20 to 30 min. Furthermore, when the zero was stopped, the data did not begin to rise until 20 or 30 min after. This sluggish behavior has a significant effect on determining the net mixing ratio for those compounds with large BG to signal ratios. Signals for mass 59 and 121 are likely due to VOCs (acetone etc.) and they are included in Fig. S3 as they respond well to zeroes.

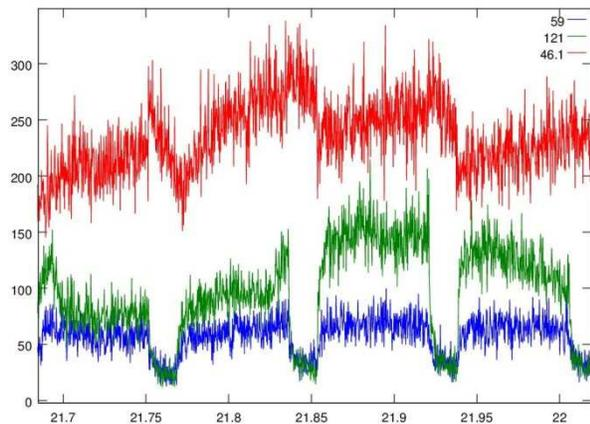


Fig. S3. Time series of signals (converted to pptv) for acetone (59u), species at 121u (possibly trimethyl benzene etc.), and dimethyl amine (46 u.) Zeroes for the VOCs are distinct and background signals are well-monitored while the dimethyl amine backgrounds are not.

The alternate BG determination is to postulate that a 'delayed' zero occurs. Data for the ten minutes after the zero was stopped was used as the BG level. So instead of discarding only the first ~13 min of data after a zero is initiated, all of it is ignored. Instead the first ten minutes of data that is usually discarded in the normal analysis is used as BG. Whether to use the normal procedure or the sluggish procedure was decided by taking the greater of the resulting mixing ratios.

Methyl and dimethyl amine mixing ratios were most affected by the sluggish behavior because of their generally low levels and relatively high BGs. Over 80% of the data for these compounds during the Oklahoma campaign was analyzed using the sluggish procedure. 70 % of the ammonia data was sluggish, while 50 % of 60 u, 74 u, 102 and 116 u amines mixing ratios were generated using the sluggish procedure. The data for the C5 amine detected at 88 u was less than 1 % sluggish due to a generally high ambient level and a low BG.

The delayed zero procedure only partially takes into account this affect: for many periods of time the data for ammonia and dimethyl amine show a rise over the ~1.5 hr time between zeroes. During these times, these species are likely to be under estimated. For most time periods when sluggishness was displayed, the data for the affected masses showed a rise to an asymptote, apparently when amine levels were stable on the hour-long time scale. The best data for these time periods and these masses are the 45 min of data just before a zero is initiated. As it is likely that the earlier 45 min is low (as much as 30 %) from the later data, the two hour averages are biased slightly lower than the actual 2 hr abundances.

Possible causes include the presence of semi-volatile carboxylic acids: the zero removes all species, bases and acids, thus the surfaces in the ionization region can release base that had been tied up by acid, causing an increase in the AmPMS signal for some amines. Once the sample flow is re-established, the acid once again suppresses base evaporation from surfaces, and this is more representative of baseline conditions for the instrument, until gas-phase amine reconditions surfaces leading to the ionization region.

Other possible explanations are: (i) Material that fell into the tee during sampling- this tee is where catalytic converter air enters AmPMS during a zero. This material could emit amines during a catalytic converter zero. (ii) If material is present on the sampling orifice disk next to, or even slightly occluding, the orifice, then reagent ions can interact with this material. (iii) Material could be accumulated near or in the ion source. Both (ii) and (iii) might cause a jump in BG signal during a catalytic zero because the reagent ion signals increase during the catalytic zero (partly due to removal of reacting species but also partly due to the small pressure change.)

Support for these three explanations comes from ions with BG signals that do not increase in the same proportion as do the reagent ion signals. There is evidence for this from ions not associated with the alkyl amines that have a large background signal. The signal at 107 u increases in Fig. S2 during a zero. Signals at other masses (124 u and 152 u) were at times quite large and were also observed to significantly increase during the catalytic zero. These three masses had signals that showed no net mixing ratios and the BGs were quite variable. Their presence as BG signals was believed to be due to material that had accumulated in the ion drift region.

S11.3 Amine Scrubbing with acid-doped tubing.

An alternate procedure for determining the background signals was used for outdoor air sampled in November, 2013 in Minneapolis. Two acid scrubber tubes (i.e., denuders) were prepared: a 30 cm length of Teflon tubing immersed in 6 M H_2SO_4 solution for several minutes, and a 70 cm length of tubing immersed in a 20 % phosphoric acid solution. The tubes were allowed to dry after the immersion (no rinsing) in a clean flow of nitrogen, and they were used to obtain BGs for the alkyl amines. In between catalytic zeroes, the sulfuric acid tube was manually placed in line with the sample gas for a period of time. To test over longer periods of time with the acid scrubbers, the three way valve was put in its original place just before the AmPMS inlet, and the sample gas was diverted through the scrubbers before entering the drift region. The results of a series of 30 cm acid scrubber experiments showed that zero levels for ammonia and amines were similar to the catalytic zero with perhaps the exception of the heavier amines, from 88 to 116 u. The heavier amines may not have been removed as efficiently by the scrubber due to slower diffusion to the scrubber wall.

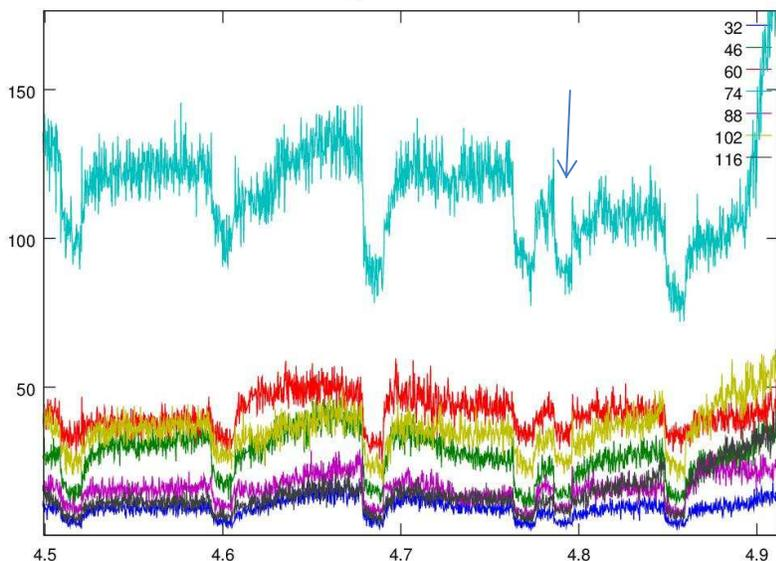


Fig. S4. Amine mixing ratios vs. fractional day for AmPMS sampling urban air (Minneapolis, MN, 2103Nov04.) Zero levels have not been subtracted from the data. The regular (2.03 hr = 0.085 d interval) catalytic zero and the scrubber zero at 4.79 d (arrow) are in good agreement. The ammonia signal behaved similarly. Net amine signals range from a few pptv to a few tens of pptv.

The second series of tests using the automatic zeroing procedure where the sample gas is periodically diverted through the acid scrubbers is shown in Figures S5, a plot of net mixing ratios for the alkyl amines from the 18th to the 25th of November, 2013. At 19.53 d, the sampling arrangement was changed from catalytic converter zeroing to sampling through the three-way valve with diversion through the scrubber tubes for BG

determination every ~2 hrs. There was an initial conditioning period of the three way valve that lasted until about 19.8 day. Initially, the 30 cm sulfuric acid coated tube was used as the scrubber. On the 20th, this was changed over to the 70 cm phosphoric acid scrubber tube (at 20.4 day.) At 22.64 days, the scrubber tube zeroing procedure was terminated and the catalytic converter zero was re-established: the three way valve was returned to its position downstream of the catalytic converter.

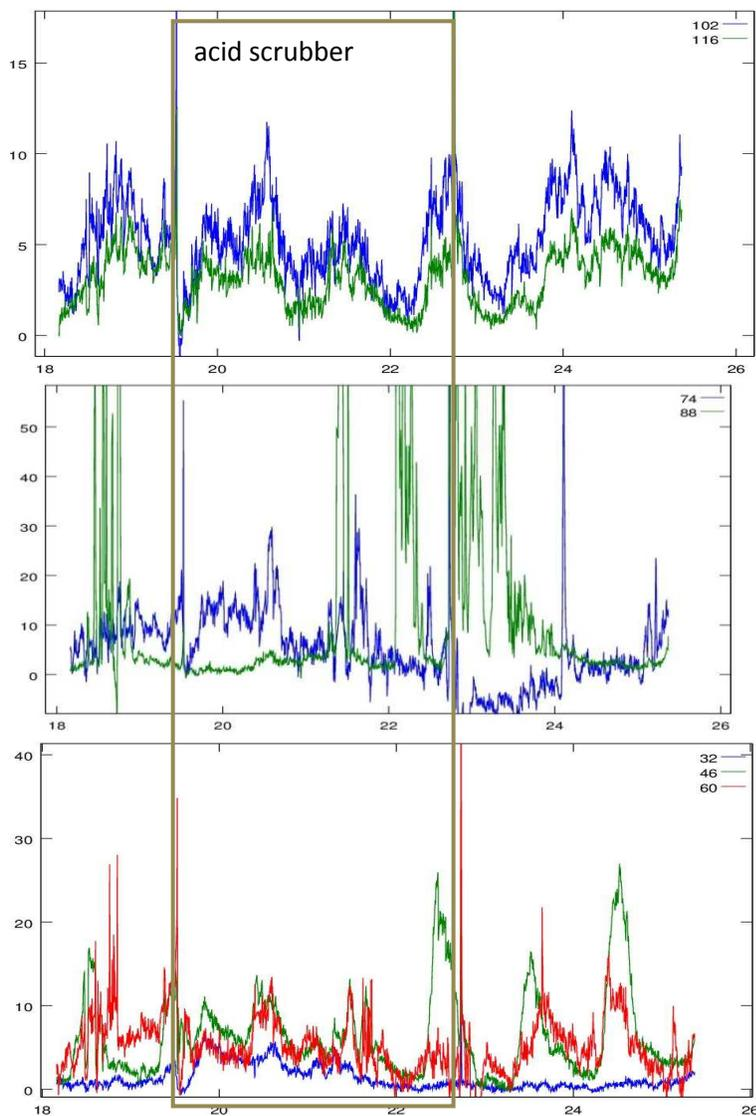


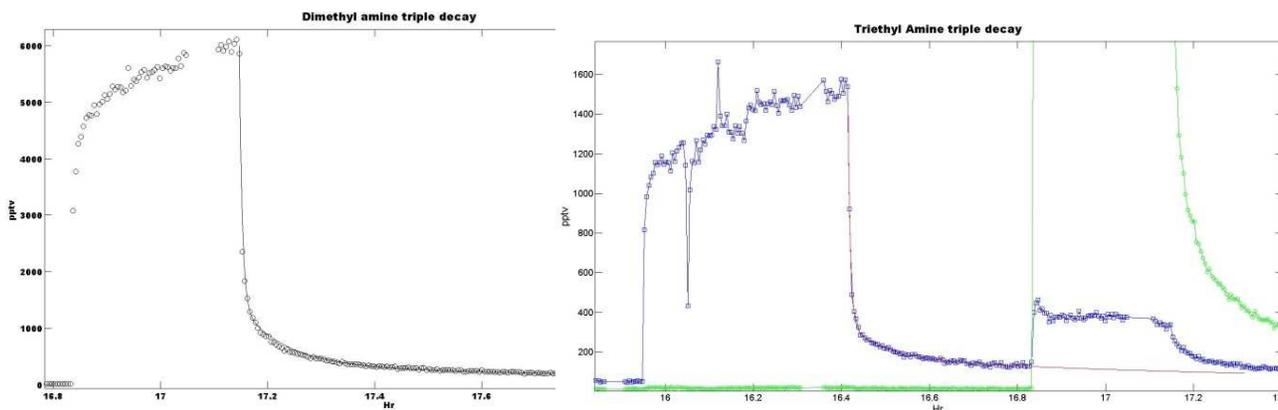
Figure S5. Mixing ratios vs. day (Nov, 2013, Mpls.) for (a) methyl, dimethyl, and trimethyl amines, (b) C4 and C5 amines (or C3 and C4 amides) and (c) C6 and C7 amines (or C5 and C7 amides). Between 19.73 and 22.75 day an acid scrubber tube was used to obtain instrument zeroes. Before and after that, the catalytic converter zero was used.

The mixing ratio data (pptv in the figure) show no discernible difference for the alkyl amines whether using the acid scrubbing tube or the catalytic converter zero, with the exception of mass 74. Interestingly, the net signal for 74 was negative for about a day when the catalytic converter zeroing procedure had been restarted. Note that the three way valve had been exposed to outdoor air for about three days previous to this and could have become a non-negligible source for the amine at 74 u. An amine mass spectrometer, recently described by Yu and Lee (2012), has also used a silicon phosphate/ H_3PO_4 scrubbing technique, such as used for ammonia (Nowak et al. 2006). The results depicted in the figure show that the acid scrubber deployed here acts similarly to the catalytic converter zeroing procedure and also likely similarly to the silicon phosphate scrubber of those researchers.

SI 1.4 Response times

An effect related to that detailed above is the interaction of amines with conditioned surfaces in AmPMS. Two experiments are detailed in Fig. S6a and b with (a) dimethyl amine and (b) triethyl amine added to humidified (~30% RH) clean nitrogen into a short sample line (30 cm) before entering the inlet to the drift region of AmPMS. Also shown in the figures are triple decay curves with time constants of 0.33 min, 5 min, and 1 hour. The relative contributions of these three curves are 70 %, 20 % and 10 %, respectively. In Fig. S6b the dimethyl amine spike (green) is shown and during this time some triethyl amine is carried in from the ~ 30 cm length of sampling lines and teflon tee and/or driven off of surfaces within AmPMS.

Fig. S6. Addition and quick removal of (a) dimethyl amine and (b) triethyl amine to AmPMS. The degassing of triethyl amine from surfaces (both internal to AmPMS and the lines leading up to it) is apparent during the DMA addition at 16.83 hr. Note that the triethyl amine permeation tube has not been quantified and these 'spikes' were not calibrations.



We observed that the method in which the flow from the permeation tube was introduced into the sample flow was important for the calibrations. The best performance was when the entire sample flow was directed over the permeation tube as was done for the majority of the calibration results presented in Table 2 of the paper. The data depicted in S6a and b were performed by tee-ing into the sample flow with a small (~40 sccm) flow from the permeation tube: often, the full amount of amine was not delivered to AmPMS and also degassing effects were larger after another amine was swapped in, such as at 16.85 hr in S6b.

In some cases it appears that ammonia is worse than the amines in terms of sticking. Shown in Fig. S7 is an experiment where ammonia and dimethyl amine were introduced to the AmPMS sample line via tee-ing into it with the exit of the dilution system. A zero occurred at 13.7 to 13.8 Hr and at ~ 14 hr the dilution system was taken off the mixing tee and replaced with a plug. While both DMA and NH_3 responded quickly to a zero, reflecting rapid response within the AmPMS drift region, NH_3 decayed much more slowly than DMA after the dilution system was removed, indicating sticking of NH_3 on the Teflon lines preceding AmPMS.

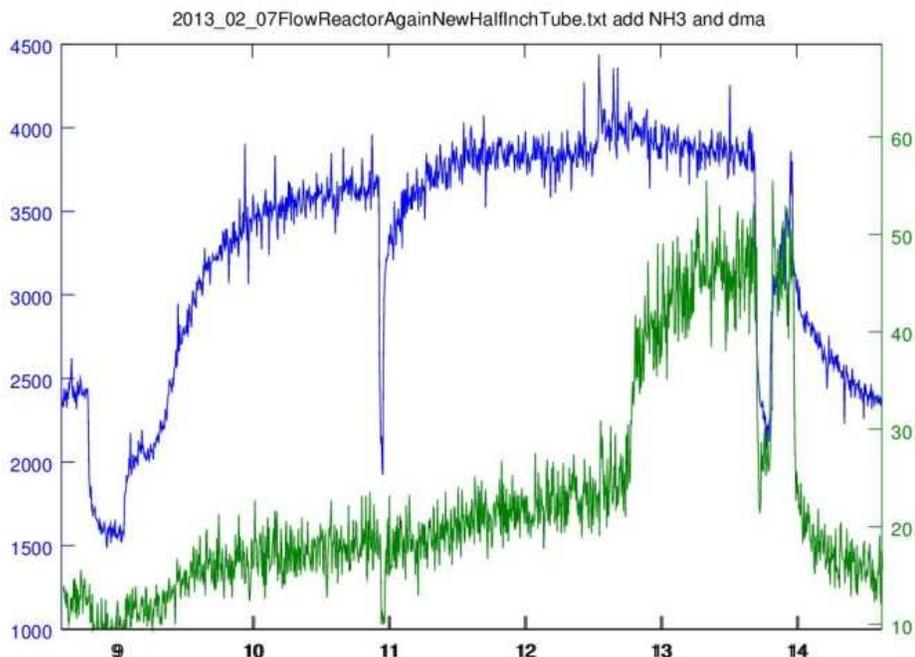


Fig. S7. Co-addition of DMA and NH₃ to AmPMS. Addition was started at about hour 9, the DMA content was increased at about hour 12.67, and the dilution system was removed from the sample flow at about 13.9 hr. The tail in the NH₃ data indicates a significant degassing from surfaces, likely upstream of the ion drift region, that dimethyl amine was not subject to.

SI 1.5 Sample line test.

A series of experiments were performed by adding an amine (a spike) at the upstream end of a 3.75 m length of 0.48 cm ID Teflon (PFA) tubing. This tubing was used in the field missions in both Lewes and in Oklahoma. About 20 % of the amine from the permeation tubes was added to the ~ 1 sLpm sample flow of outdoor air in Minneapolis resulting in spikes of about 2000 pptv of methyl or trimethyl amine for a time period of 20 to 45 min.

Shown in the plots below are mixing ratios of the amines for three cases of amine spikes: (i) bypassing the 3.75 m sample line, (ii) into the 3.75 m sampling line that had been rinsed with deionized water after the Oklahoma campaign and then used for about 5 weeks of sampling urban air in Minneapolis (2 weeks in July 2013 and 3 weeks in Oct and Nov 2013) (iii) after the sampling line was rinsed with hot tap water, ultrasonically cleaned with a dilute Alconox soap solution, rinsed with hot tap water, rinsed with a ~0.5 l of deionized water, rinsed with a few hundred mL of a ~0.01 M sodium bicarbonate solution and then dried after removing most of the droplets from the baking soda rinse. Leftover from the Oklahoma campaign was a small amount of web-like material, perhaps the start of a cocoon. It was near the upstream end of the sample line and it was not fully removed by the cleaning procedure.

The duration of the spikes was not uniform and the comparison of amine stickiness is depicted by the decay behavior after the amine addition was stopped. Thus time zero for each of them was selected to be when the amine spike was terminated. The amine signals quickly rise upon introduction, except for the methyl amine spikes into the 3.75 m sampling line (clean and dirty) which were quite delayed from the -0.9 (dirty) and -0.35 hr (cleaned) initiations. For the four experiments that showed a quick response, a slower rise to about 2000 pptv is evident at which time the spike was terminated by removing the PT assembly from the sampling line.

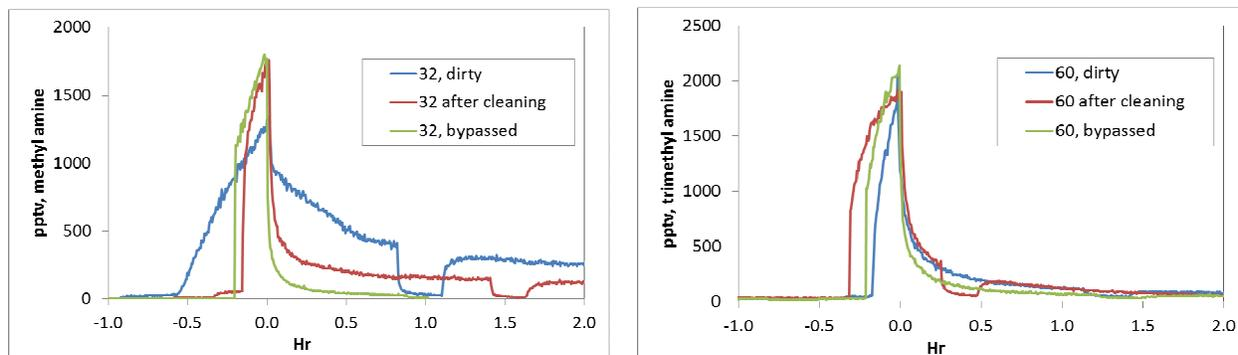


Fig. S8. Rise and decay of methyl amine (a) and trimethyl amine (b) spikes to AmpMS sampling lines for various conditions.

There is a noticeable interaction of the amines with the sample line, especially methyl amine with a sample line that had been exposed to a large volume of outdoor air. Interestingly, trimethyl amine was much less affected by the dirty sampling line. Nonetheless, the data indicates that the sampling line absorbs amines, ‘passivates’ to this high level on the ten minute time scale, then releases the absorbed material over the next 1 hr (trimethyl amine) to 3 hr (methyl amine.) Catalytic converter zeroes were initiated during the experiments and are easily picked out in the figure, confirming that the source of the ‘extra’ amine is the sample line.

It appears that the amount of amine added was fully recovered so the effect of the sampling tubing is to smear out in time changes in ambient amine levels. Therefore the data, represents some sort of average of the preceding 10 to 30 minute ambient amines. It is likely that the larger amines act similarly to the behavior of trimethyl amine where the interaction with the sampling line is muted compared to MA: perhaps a ten minute time lag is appropriate for an 80% decrease in amine to be registered by the system. Since the behavior of dimethyl and triethyl amines is similar, as depicted in Fig. S4a and b, it is probable that dimethyl amine acts similarly to trimethyl amine and the larger amines. Ammonia and methyl amine appear to have a larger interaction with the perfluorocarbon tubing. For these reasons and because of the sluggish behavior of the zeroes, the data sets for both Oklahoma and Lewes are reported as ~ 2 hr averages (some of the later Lewes data is hourly due to more frequent zeroing.) It is likely that many of the amines have a quicker response than these 2 hr averages suggest.

SI1.6 Low ion count rate episodes.

There were episodes during the OK field study where the instrument had very low reagent ion count rates and its absolute detection sensitivity had been debilitated. Some calibrations for methyl amine and DMSO were taken when the instrument had been in one of these episodes. These episodes occurred, presumably, when there was a clog in the ion entrance orifice (e.g., dust or fiber) that lead to large reductions in ion signals (up to 97 % decrease in $s_0 \sim 3000$ Hz). In these cases, the relative sensitivities for CH_3NH_2 and DMSO, ratioed to S_{typ} , appeared to increase to 3 and 6, respectively, much greater than for nominal conditions. After these anomalous calibrations were performed, the orifice clog disappeared when a very hot catalytic converter (660 °C) was placed in line with the sample gas; the data shown in Table 2 of the paper were taken when signals had returned to normal levels, $s_0 \sim 100$ kHz. The amount of signal loss was variable in the field campaign, reflecting variability in the position of the ion beam and perhaps also orifice blockage. When s_0 was reduced by more than 95 %, the relative sensitivities were probably greatly affected. Therefore, ambient measurements were deemed reliable when losses in s_0 were less than 95 % (e.g., $S_0 > 5$ kHz.) Some calibrations were performed at ~ 90 % loss reagent signal and were comparable to the normal reagent ion signal calibrations.

SI.2 Calibration of AmpMS with VOCs

DMSO was detected in Lewes DE by AmpMS; it has a large proton affinity and detection by mass spectrometry has been reported by Nowak et al. (2001). A DMSO PT was fabricated and its permeation rate was determined by comparing it to an evaporation calibration of a PTrMS (see below). Detection of DMSO by AmpMS was primarily as $\text{DMSO}\cdot\text{H}^+$ at 79 u but a signal at 96 u due presumably to the $\text{DMSO}\cdot\text{NH}_4^+$ ion, tracked the signal at 79 u. This is depicted in the figure below where the signal ratio of 96 u to 79 u is plotted against the signal ratio of 18 u to that of the water proton clusters (19 u, 37 u and 55 u). Evidently, DMSO reacts with $\text{NH}_4^+\cdot(\text{H}_2\text{O})_n$ clusters and retains the NH_3 ligand to some extent.

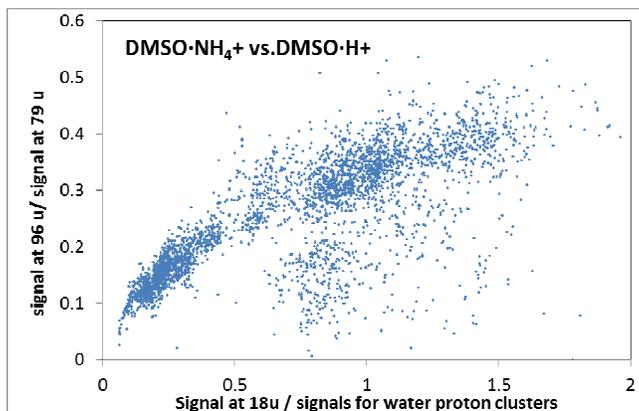


Fig. S9. Signals due to DMSO reacting with water proton clusters and ammonium clusters (18u).

SI.2.1 DMSO quantification.

A DMSO permeation tube was quantified by comparison to a calibrated PTrMS (Hanson et al. 2009). The PTrMS was calibrated for DMSO by the evaporation method. In the PTrMS calibrations (two evaporation trials are shown in Fig. S10), the DMSO signal at $\text{M}\cdot\text{H}^+$ (79 u) was accompanied by signal for dimethyl sulfone (DMSO_2) at $\text{M}\cdot\text{H}^+$ = 95 u. DMSO is a sticky molecule and is retained for some time on the PTrMS sampling lines and within the ion drift tube. When it is stuck on the surfaces in the drift tube it is exposed to OH radicals from the glow discharge ion source. DMSO residing on the inner surface of the drift tube is apparently readily oxidized to DMSO_2 (A. Wisthaler, private communication, 2013) and perhaps other species: e.g., the main gas-phase product is methane sulfinic acid (**S29**). The sum of the signals at 79 u (37%) and 95 u (63%) were used to obtain sensitivities and to transfer these sensitivities to quantify the permeation tube; if DMSO oxidizes to any other species, then the permeation rate is underestimated.

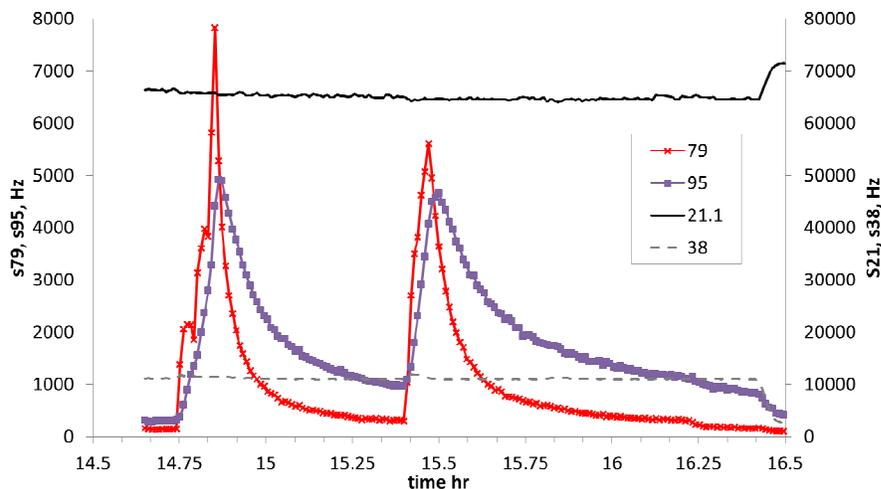


Fig. S10. PTRMS signals due to DMSO and its oxidation products within the PTRMS instrument. Two evaporations of μL quantities of mM DMSO solutions into a carrier gas sampled by the instrument are shown.

When the DMSO permeation tube was used to calibrate AmPMS, there was no signal observed at 95 u. This is consistent with low amounts of OH exiting the radioactive ion source of AmPMS (vs. the PTRMS' glow discharge source) and the much lower sticking observed for DMSO when introduced into AmPMS. Note that the DMSO permeation rate is uncertain due to potentially undetected oxidation products inside the PTRMS drift tube. To remedy this situation, gravimetric determination of the DMSO permeation rate and DMSO evaporation calibrations of AmPMS are planned.

SI3. Other ions observed in Lewes campaign.

There were a number of ions that do not correspond to alkyl amines that were monitored at each site. They are difficult to assign to any particular species and thus have unknown sensitivities however, assuming efficient proton transfer, observed net signal can be converted to mixing ratio using S_{typ} . A few ions with interesting behavior observed at Lewes DE are depicted in the figure below along with the signals due to DMSO. If they are due to species with amino groups they are likely to be detected quite efficiently (i.e., appropriate to convert signals to mixing ratios assuming S_{typ} , left axis.) Early in the campaign, sp168 (the species detected as 168 u) was generally quite low while sp186 was at times 40 pptv. Later on in the campaign, they were at comparable levels and well correlated; they were generally high during the night and low during the daytime. Except for perhaps pyridine (80 u, with a little spillover from C-13 DMSO), these species cannot be readily identified and it is possible that the signals represent more than one species: among a number of species, 168 u could be protonated ring amine compounds species such as carbazole or cyclohexyl piperidine or oxidized species such as dipicolinic acid and methoxyanthranilic acid. This is an example of some of the additional ions besides those due to the alkyl amines that can be monitored using AmPMS.

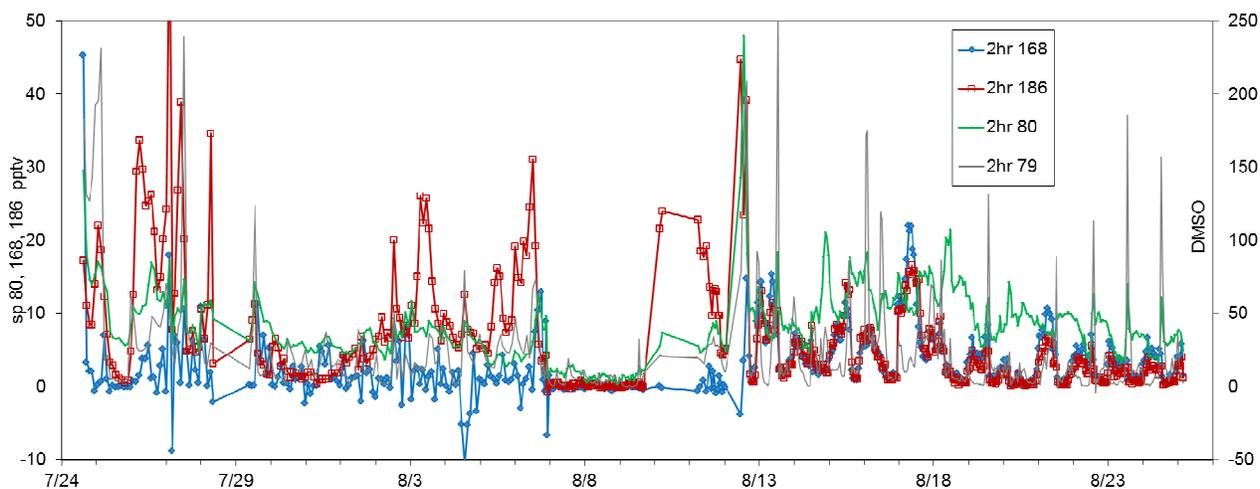


Fig. S11. Species due to ions detected at 80, 168 and 186 u along with 79 u (right axis, due to DMSO.) Signals converted to mixing ratio, pptv, assuming S_{typ} .

SI4. Diurnal hourly means, medians and percentiles.

Discussed in the text are the diurnal behavior of the medians for amines and ammonia from Oklahoma. Shown below are the plots for ammonia (18 u), methyl amine (32 u), and dimethyl amine (46 u) are in the left hand plots; C3 amine (60 u), C4 amine (74 u) and C5 amines (88 u) are in the middle plots, and C6 and C7 amines are on the right. Data are plotted as mixing ratios (in pptv) against hr of the day. The 25th and 75th percentiles are also depicted.

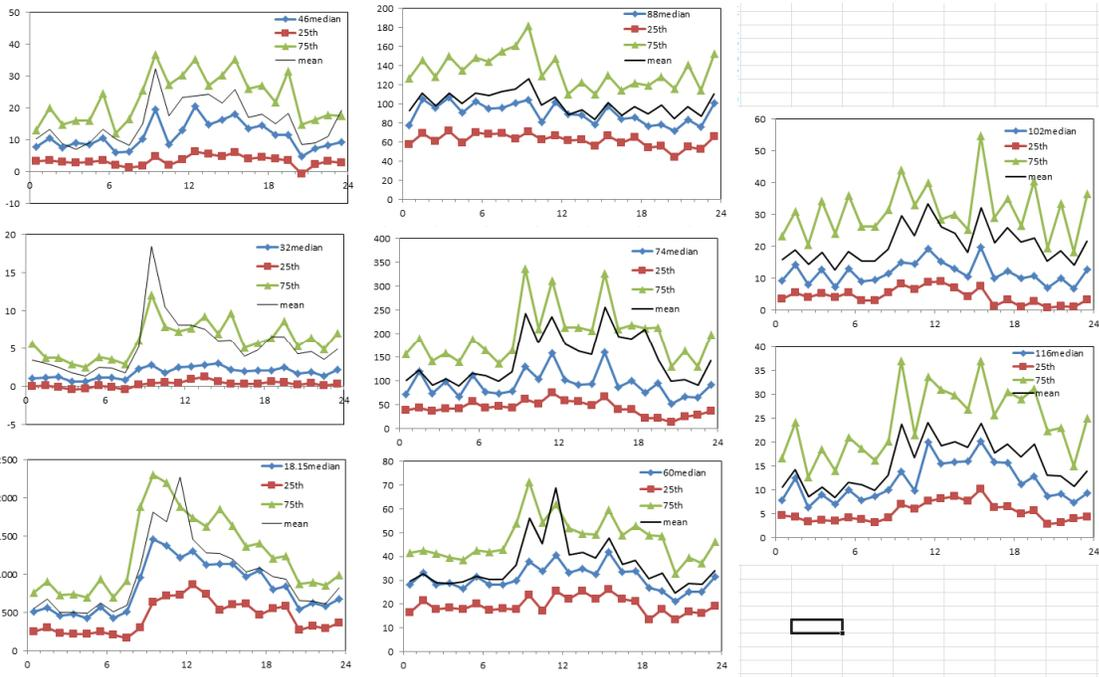


Fig. S12. Diurnal hourly mean, median and 25th and 75th percentiles for ammonia and the amines detected in Oklahoma, Spring 2013.

S15. Correlations from Lewes

Ammonia, methyl, dimethyl and trimethyl amine data from Lewes are shown in correlation plots below (Fig. S13). Methyl and dimethyl amines are well correlated, ammonia and methyl amine are somewhat correlated and trimethyl and the C7 amine are not well correlated with any amine. 60 u data is correlated with DMSO. Of all these species, ammonia shows the most significant correlation with temperature.

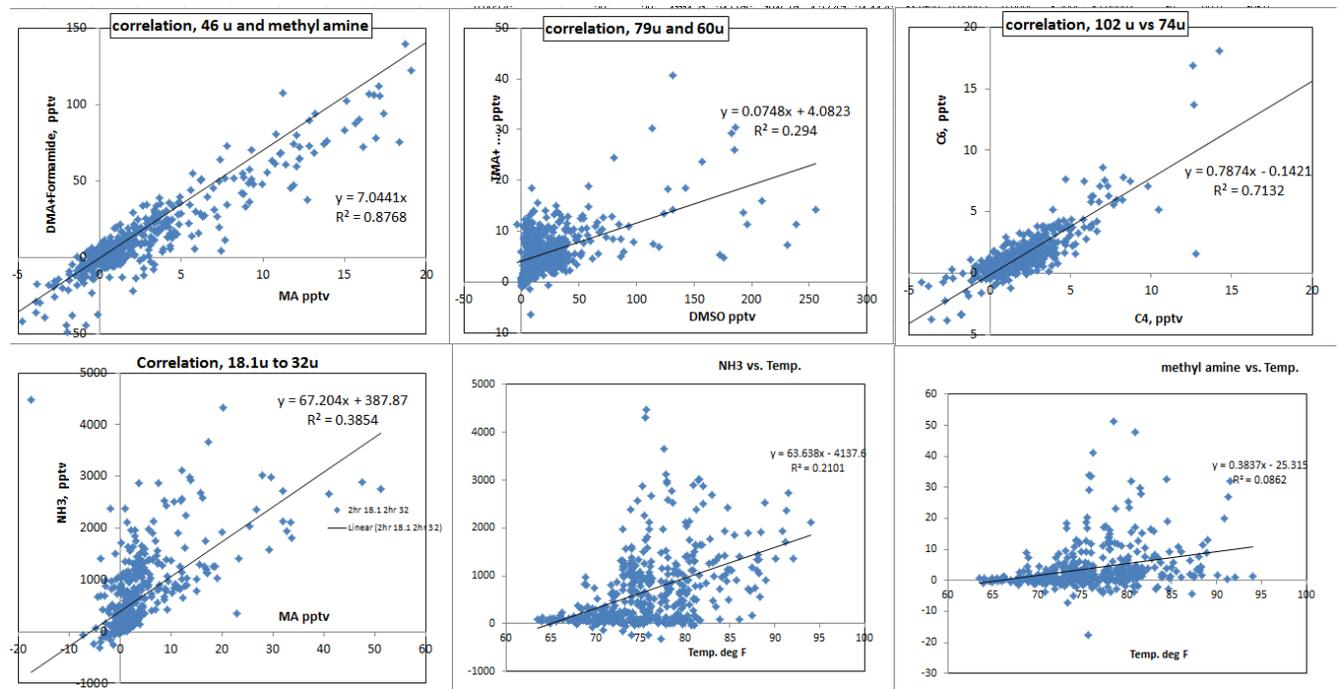


Fig. S13. Correlation plots of amines with various other species and temperature. R^2 is the square of Pearson's correlation coefficient.

S16. Addition of Base to a Flow Reactor and Computational Fluid Dynamics.

Amine levels needed for nucleation studies (Zollner et al., 2012; Kirkbby et al. 2011) are in the single to tens of pptv range. To achieve this in a flow reactor experiment operating at 3 to 4.5 mmol/s total flow, the flow from the PT was diluted in multiple stages with an overall decrease of up to 99.9% of the amine. Amine levels of several hundred pptv in a flow of ~ 50 sccm N_2 were prepared with the dynamic dilution set-up shown in Fig. S14a and delivered to the flow reactor through a sidearm (S14b) and further diluted by the total flow (6000 sccm or 4.5 mmol/s) to single digit pptv levels. Note that the flow reactor wall is coated with H_2SO_4 and is a sink for bases. Therefore, there is not a uniform [base] present after mixing; however, a useful reference is the mixing ratio calculated assuming No Loss and after Dilution (NLD). During mixing, [base] is quite a bit larger than NLD; on the other hand, near the walls or at the end of the flow reactor [base] is much less than the NLD value (Zollner et al. 2011).

Previously, ammonia or methyl amine was introduced to the flow reactor between the mixing region and nucleation region shown in Fig. S14b (Zollner et al. 2011). Without dilution of [amine], particle numbers saturate the particle counter thus the need for low levels in the nucleation region. The base level at the detection region of the flow reactor (~ 120 cm downstream) was very low due to loss to the wall. In some experiments, the dilution system was connected to a port at the bottom of the flow reactor and AmPMS signals were in agreement with that expected for NLD.

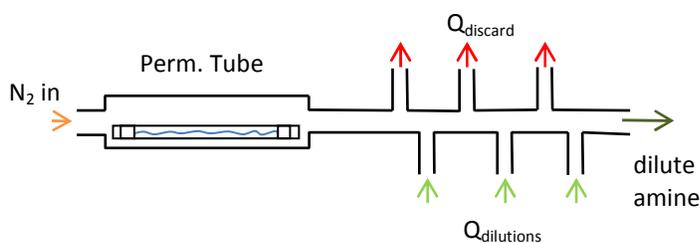


Figure S14a. Dynamic dilution set-up. Nitrogen gas is sent over the PT and then known fractions of gas are removed and then replaced by clean N_2 . The amine level is diluted several times before entering the flow

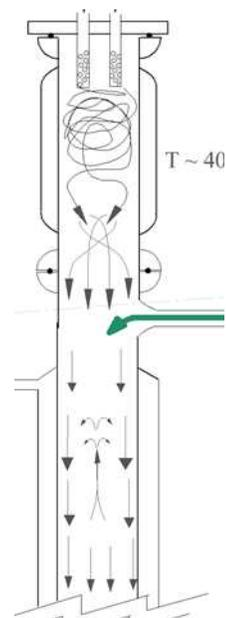


Figure S14b. Base addition port on the nucleation flow reactor. The flow from the dilution system mixes with the nearly plug and warm ($\sim 30-35$ C) flow within ~ 20 cm; simulations show that this addition eliminates much of the buoyant zone flow.

Computational fluid dynamics simulations of the mixing of the base into the main flow were performed using the 3D model of Panta et al. (2012) with the following important alterations: (i) the number of volume elements was increased from 1.4×10^5 to 2.1×10^6 , (ii) second order solvers were selected for energy, momentum, pressure and the monomers (sulfuric acid and base) and (iii) the convergence criteria for many parameters were strengthened.

Shown in Figs. S15 are contour plots of (a) ammonia addition into 6 sLpm through the top port as shown in Fig. S14b and (b,c) dimethyl amine addition to a flow of 4 sLpm near the bottom of the flow reactor. The ammonia levels shown in S15(a) agree with those of our previous fluid dynamics simulations shown in Fig. A11(II) of Panta et al. (2011): the main difference is that the improved 3D model here has the sidearm flow, and thus ammonia, better traverse into the center of the reactor. The current results are in accord with the conclusion of the previous work where it was shown that mixing is sufficiently fast such that the majority of nucleation occurs at least 10 cm downstream of the

base addition port (Figs. A12 and A13 in the Appendix of Panta et al.) The maximum in concentration 18 cm downstream of the port is about twice the NLD value; the average value across the diameter of the flow reactor is about the NLD value.

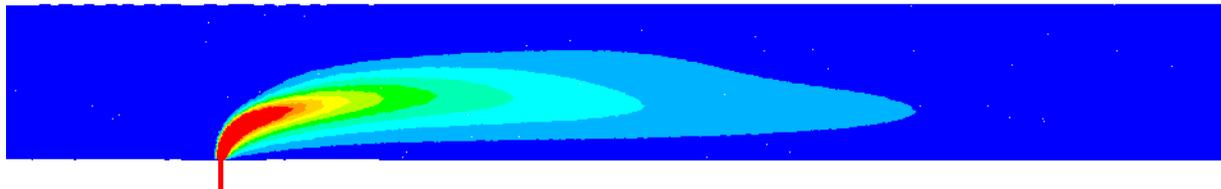
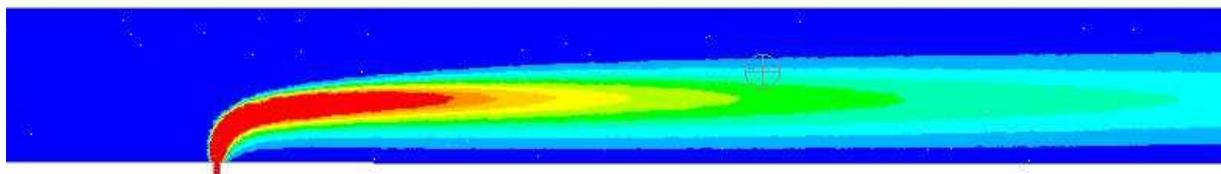


Figure S15a. Contours of ammonia (24 pptv intervals, 240 max). NH_3 in a sidearm flow of N_2 (0.05 sLpm) added to the main flow (6sLpm) that is also cooling due to interacting with the wall: from 307 K (incoming at the left) to ~ 298 K (outgoing, right.) NLM is 16 pptv. Note that ammonia is present at ppbv levels in the N_2 flow (40-100 sccm) exiting the dynamic dilution system, and it mixes down to the tens of pptv levels in the main flow.

The dynamic dilution system was also attached to the flow reactor near the flow reactor exit and just above a mass spectrometer system which monitors trace species using chemical ionization with NO_3^- or H_3O^+ core ions. (S30, S31, S32, 13) The distance between the port where the dynamic dilution system enters the flow reactor and where the mass spectrometer samples the flow is 18 cm. CFD simulations of amines, H_2SO_4 and their clusters were performed. The total flow rate in the reactor is 4 sLpm, the total flow from the dynamic dilution system is 40 sccm, the base is dimethyl amine (estimated diffusion coefficient in N_2 of $0.11 \text{ atm cm}^2/\text{s}$) and temperature is 298 K.

The results of the simulations (Fig. 15(b)) show that mixing of base into the sulfuric acid containing flow is similar to that shown in 15(a) for ammonia. The main difference is that the sidearm flow is not as penetrating in the isothermal case (15b) which is probably due to the lack of a central buoyancy that allows for more flow at the center. Nonetheless, whether the mixing occurs at the top of the reactor near a buoyant flow or into an isothermal, but smaller, flow, mixing via diffusion is relatively rapid. Reverse pathlines beginning at the center of the sampling region of the mass spectrometer and ending at the level of the base inlet show that there is about 2-to-3 s of reaction time for the 18 cm of travel. This average velocity is about twice that assuming plug flow: this is expected for the centerline flow for fully developed laminar flow.



t

Figure S15b Contours of dimethyl amine (intervals, 2.5 pptv, 25 max). Amine in a sidearm flow of N_2 (0.04 sLpm) added to the main flow (4 sLpm) for isothermal conditions (298 K.) NLM is 5 pptv.

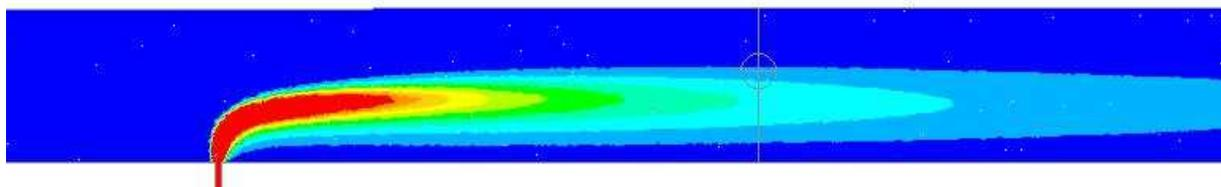


Figure S15c. Contours of dimethyl amine as in (a) but now allowing it to cluster with sulfuric acid molecules, present at ~ 50 pptv. Differences with S15b is due to uptake onto clusters.

Fig. S15c shows DMA contours allowing for reactions with sulfuric acid. It shows that at ~18 cm downstream of the port (the gray line and circle +), DMA has a maximum of 7 pptv which is about 5 pptv less than the maximum when no reaction is allowed. The reaction scheme will be presented in a manuscript under preparation (**S33**). The no-loss mixing ratio (NLD) for his simulation is 5 pptv. The simulation shows that sulfuric acid is about 50 pptv in this region of the flow reactor: sulfuric acid is also lost on the reactor wall and has a maximum value on the central axis of the flow reactor.

S17. Permeation Tube and Titration Information.

Shown in Fig. S16 is a schematic diagram of two small flasks (in tandem arrangement) with stirring bars, pH probes, and bubbling permeation tube gases. Stirring enhances the presence of acid at the surface of the bubbles, ensuring better transfer of base gas into solution. Flow rate of N₂ over an NH₃ permeation tube was varied from 5 up to 40 sccm and there was no noticeable effect on the measurements.

S17.1 Tandem titration

Figure S17 shows data from a tandem titration where base absorption rates for both flasks are shown. The first solution (red) shows an NH₃ absorption rate (13 pmol/s, ~2 year old PT) while the second solution (black) absorption rate is much lower (0.7 pmol/s) during this time. These data indicate that the first flask captures 95 % of the base molecules in the flowing gas. Blank runs (without a PT) showed generally low but at times quite variable neutralization rates: as low as 0.5 pmol/s and as high as 3 pmol/s; sometimes the initial (first 1000 s) neutralization rate was even larger. Absorbed base on silicone sealing materials and Teflon components are believed to be responsible for this artifact neutralization. The high rates were traced to previous exposure to base at high levels: thorough cleansing of the entire apparatus was important. Therefore, the carryover from the first flask for pH < 6 is probably less than 5 % and no correction to measured neutralization rates have been made for this effect.

After the first solution had been neutralized, the rate of absorption by the second flask slowly increased and reached a maximum of ~4 pmol/sec. This delay and the overall slower neutralization rate were due to the saturation of the first solution according to NH₃'s Henry's law solubility after the acid had been used up. The time delay in the pH changes in the second solution is roughly in accord with an estimated time constant for Henry's law saturation of the first solution, $\sim 1 \times 10^5$ s, given by the quantity $HRTV/F$ where H is the Henry's law constant (60 M/atm(**S34**)), R is the gas constant, T is temperature, V is the volume of the solution and F (~22 cm³/min) is the volumetric flow rate of the PT assembly.

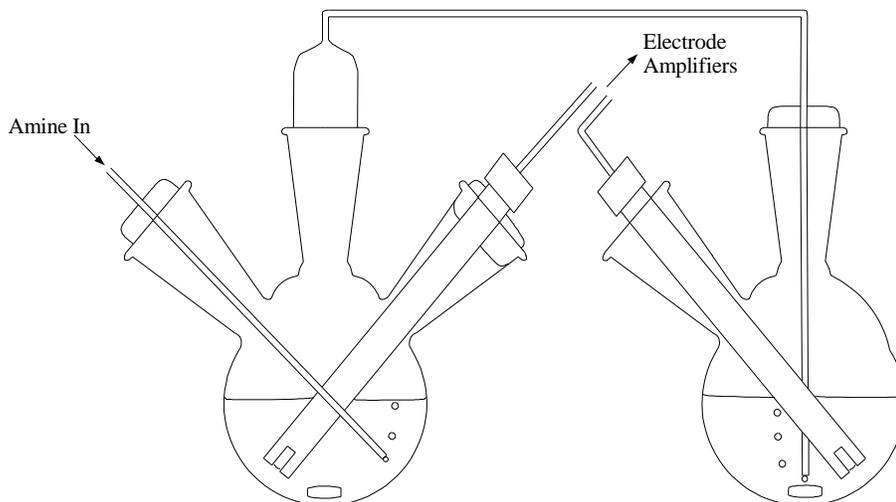


Figure S16. pH measurement apparatus. Effluent from perm tube at 20 sccm is bubbled through a stirred 40 mL solution initially at pH 5. Tandem apparatus is shown for assessing carryover; generally these two flasks are run in separate experiments and two amine PTs can be calibrated simultaneously.

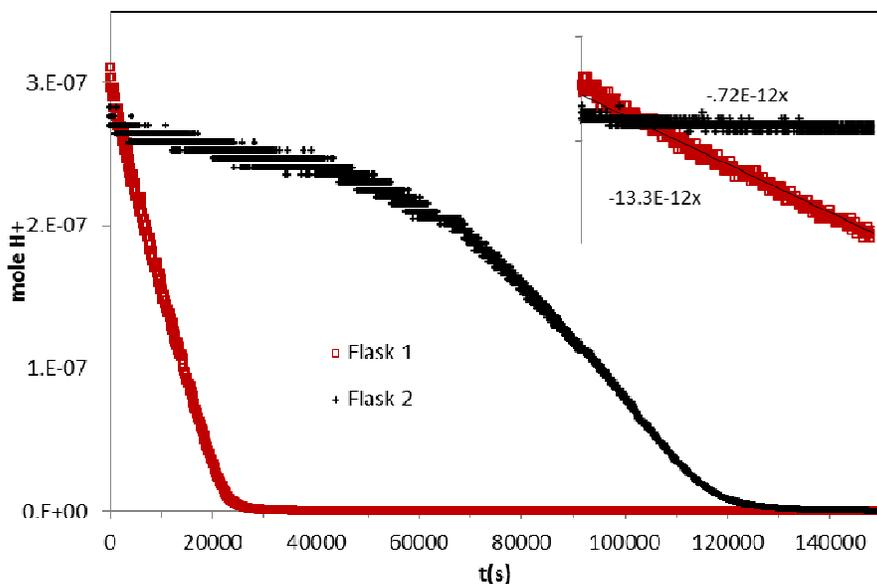


Figure S17. A tandem titration of an NH_3 PT. Mole H^+ vs. time where red squares represent the first flask and the black symbols (+) represent the second flask. The initial 10000 s are shown in the inset.

S17.2 Time and Temperature dependence of Permeation Rates

The change in the permeation rate with time of a newly constructed dimethyl amine PT was investigated and after about two weeks the permeation rate had stabilized (Fig. S18). This may be a common behavior for our PTs and it is probably due to the time that is needed for the steady state flux through the wall of the PT to be established. It may also be due to chemical conditioning of the plastic. We observed that rates for older (> 6 months) PTs decreased steadily over time (Fig. S19), possibly through depletion of the amine inside the tube. Water also probably permeates from the tubes for those amines in aqueous solutions and thus changes in composition over time may occur which may be

responsible for some of the time dependent permeation rates. The amount of water loss was not assessed.

Frequent calibrations are necessary to capture the day-to-day variability in the permeation rates. For the mature PTs depicted in Fig. S19, the exponential fits to the amine PTs are included to guide the eye rather than to explain the data. The several month old NH_3 PT in Fig. 7 had a perm. rate of 120 pmol/s which decreased to 60 pmol/s over ~3 mos. and over the next 5 mos. its perm. rate varied between 50 and 80 pmol/s. It has a rather large day-to-day variability that is about $\pm 25\%$ (the very large value at ~220 d was when the room was quite warm.) The very mature DMA PT in the figure had a rate that decreased from 15 to 6 pmol/s over 120 days - a rather quick secular change and this PT was taken out of service. MA decreased from 40 to 20 pmol/s over a 100 day period but it became more stable over the next few months at 12 to 15 pmol/s. Making titration calibrations a routine component of PT work is important.

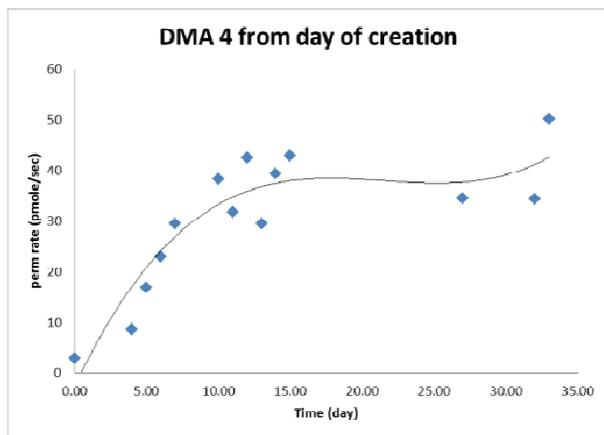


Fig. S18. Permeation rate of a dimethyl amine PT in its first month. Rate stabilized in about two weeks; a mature PT is considered to be one of 1 month age or longer. Perm. rates of mature PTs generally decline slowly with time.

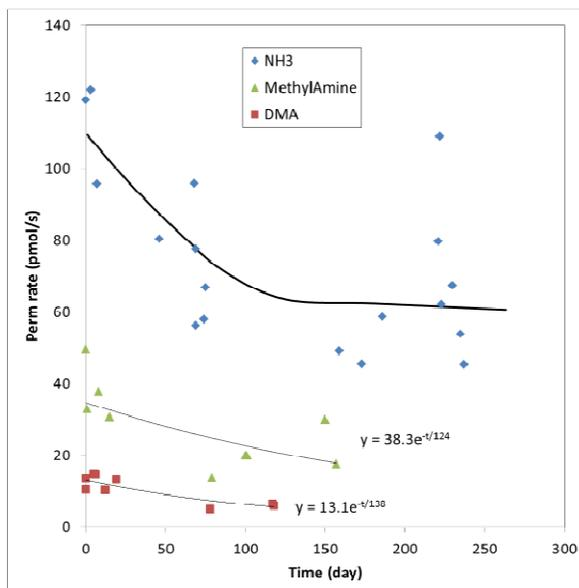
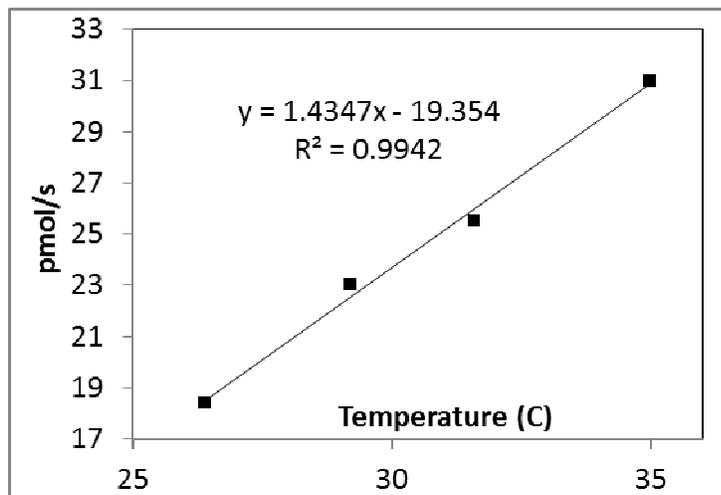


Figure S19. Permeation rates of mature PTs over the course of several months. The lines are drawn to guide the eye and for the amines are exponential decays. The scatter in measured permeation rates can be quite large day-to-day.

Shown in Fig. S20 are permeation rates for a mature NH_3 PT as a function of temperature. A linear relationship with temperature explains the dependence adequately. Near $30\text{ }^\circ\text{C}$, the rate increases about 6 % per $^\circ\text{C}$; this is close to that measured for deuterated acetone(16). Another experiment with a different NH_3 PT showed a similar temperature dependence. The PT's time at each temperature was a few to several hours and it is possible that more time is needed to fully establish steady state permeation rates. Nonetheless, this temperature dependency may adequately represent the changes in permeation rates when temperature changes occur on the time scale of several hours.

Certainly part of the day to day variability in Figs. S18 and S19 is due to changes in room temperature which was generally noted to be within 3 ° of $25\text{ }^\circ\text{C}$. PT temperature since then has been routinely recorded along with pH measurements. Temperature stability of the PT during its use is also important. There are some titration experiments where the pH probe had not been recently calibrated and a drift of up to 0.15 pH units in the probe response was noted. This would lead to an error of up to 40 % for these isolated experiments. Calibration of the probe for each titration and checking it post titration is now routine. As discussed above, titrations starting at higher acid content (pH of 4.3 or so) show less variability.

Figure S20. Changes in NH₃ permeation rate with variations in temperature. Increase in permeation rate is approximately linear in this small temperature range.



References for SI.

S29. Arsene, C., Barnes, I., Becker, K.H., Schneider, W.F., Wallington, T.J., Mihalopoulos, N. and Patroescu-Klotz, J. Formation of Methane Sulfinic Acid in the Gas-Phase OH-Radical Initiated Oxidation of Dimethyl Sulfoxide, *Environ. Sci. Technol.*, 36, 5155-5163, 2002.

S30. Hanson DR, Lovejoy ER. Measurement of the thermodynamics of the hydrated dimer and trimer of sulfuric acid. *J Phys Chem A*. 2006;110(31):9525-8.

S31. Zhao J, Eisele FL, Titcombe, M., Kuang, C., McMurry PH Chemical ionization mass spectrometric measurements of atmospheric neutral clusters using the cluster-CIMS, *J. Geophys Res.*, 2010; 115, D08205.

S32. Jen C, Hanson DR, McMurry PH. Stabilization of the H₂SO₄ dimer by amines, submitted to *J. Geophys. Res.*, 2014.

S33. Glasoe WA, Panta B, Volz K, Hanson DR et al.: Sulfuric acid: A systematic study of amines and experimental nucleation rates, in preparation, 2014.

S34. Clegg SL, Brimblecombe P. Solubility of ammonia in pure aqueous and multicomponent solutions. *J Phys Chem*. 1989;93(20):7237-48.